J Pharmacol Sci **110**, 295 – 305 (2009)

Journal of Pharmacological Sciences

Full Paper

Effects of Ranolazine, a Novel Anti-anginal Drug, on Ion Currents and Membrane Potential in Pituitary Tumor GH_3 Cells and NG108-15 Neuronal Cells

Bing-Shuo Chen[1,2], Yi-Ching Lo[3], Hsung Peng[4], Tai-I Hsu[4], and Sheng-Nan Wu[1,4,*]

[1]*Institute of Basic Medical Sciences,* [4]*Department of Physiology, National Cheng Kung University Medical College, Tainan 70101, Taiwan*
[2]*Department of Anesthesiology, Buddhist Dalin Tzu Chi General Hospital, Chiayi County 622, Taiwan*
[3]*Department of Pharmacology, Kaohsiung Medical University, Kaohsiung 807, Taiwan*

Received January 16, 2009; Accepted May 11, 2009

Abstract. Ranolazine, a piperazine derivative, is currently approved for the treatment of chronic angina. However, its ionic mechanisms in other types of cells remain unclear, although it is thought to be a selective blocker of late Na^+ current. This study was conducted to evaluate the possible effects of ranolazine on Na^+ current (I_{Na}), L-type Ca^{2+} current ($I_{Ca,L}$), inwardly rectifying K^+ current ($I_{K(IR)}$), delayed-rectifier K^+ current ($I_{K(DR)}$), and Ca^{2+}-activated K^+ current ($I_{K(Ca)}$) in pituitary tumor (GH_3) cells. Ranolazine depressed the transient and late components of I_{Na} with different potencies. This drug exerted an inhibitory effect on $I_{K(IR)}$ with an IC_{50} value of 0.92 μM, while it slightly inhibited $I_{K(DR)}$ and $I_{K(Ca)}$. It shifted the steady-state activation curve of $I_{K(IR)}$ to more positive potentials with no change in the gating charge of the channel. Ranolazine (30 μM) also reduced the activity of large-conductance Ca^{2+}-activated K^+ channels in HEK293T cells expressing *α-hSlo*. Under current-clamp conditions, low concentrations (e.g., 1 μM) of ranolazine increased the firing of action potentials, while at high concentrations (≥10 μM), it diminished the firing discharge. The exposure to ranolazine also suppressed I_{Na} and $I_{K(IR)}$ effectively in NG108-15 neuronal cells. Our study provides evidence that ranolazine could block multiple ion currents such as I_{Na} and $I_{K(IR)}$ and suggests that these actions may contribute to some of the functional activities of neurons and endocrine or neuroendocrine cells in vivo.

Keywords: ranolazine, Na^+ current, inwardly rectifying K^+ current, GH_3 cell, NG108-15 cell

Introduction

Ranolazine is a derivative of lidocaine with its *N*-diethyl group cross-linked by an amine group to form a piperazine ring. It is currently approved to be a new anti-ischemic drug for the treatment of chronic angina or arrhythmic disorders (1). Its underlying mechanism of actions in angina and cardiac arrhythmias is thought to be due to the selective inhibition of late Na^+ current (2 – 6). It has been recently demonstrated that ranolazine can block muscle $Na_V1.4$- and neuronal $Na_V1.7$-channel isoforms expressed in HEK293T cells in a state-dependent manner (7). Previous studies have shown that some of agents known to alter the kinetics of sodium channels can activate Ca^{2+}-activated K^+ current ($I_{K(Ca)}$) (8, 9). However, little information is available regarding the underlying mechanism of actions of ranolazine on ion currents or membrane potential in neurons and endocrine or neuroendocrine cells.

The *ether-à-go-go*-related-gene (*erg*) (or K_V11) channels, which are encoded by three different gene subfamilies, are characterized by slow activation and fast inactivation kinetics as compared with classical K_V channels. The channel can give rise to the inwardly rectifying K^+ current (i.e., $I_{K(IR)}$) with rapid inactivation kinetics that results in an inward rectification (10). This current present in endocrine cells, such as GH_3 cells, pancreatic β-cells, and adrenal chromaffin cells, can

*Corresponding author (affiliation #4). snwu@mail.ncku.edu.tw
Published online in J-STAGE
doi: 10.1254/jphs.09018FP

contribute to the maintenance of the resting potential and thereby influence the discharge frequency of action potentials (APs). As a result, such K^+ channels are responsible for the stimulus-secretion coupling of these cells (10 – 14). Previous reports showed the ability of risperidone or ceramide to suppress $I_{K(IR)}$ in pituitary GH_3 cells (14, 15). Pharmacological blockade of this current in the CNS has been recently noted to result in changes in neuronal excitability that would alter synaptic integration (16, 17). Alternatively, several studies reported that ranolazine can block the human *ether-à-go-go*-related gene (HERG) K^+ current expressed in *Xenopus* oocytes and in HEK293 cells (18, 19). It would thus be interesting to determine the ability of this drug to block $I_{K(IR)}$ in neurons and endocrine or neuroendocrine cells.

Therefore, in this study, we attempted to determine the mechanism by which ranolazine interacts with ion currents [i.e., voltage-gated Na^+ current (I_{Na}), L-type Ca^{2+} current ($I_{Ca,L}$), $I_{K(IR)}$, delayed rectifier K^+ current ($I_{K(DR)}$), and $I_{K(Ca)}$] to cause any effects on membrane potential in pituitary tumor (GH_3) cells. The results revealed that ranolazine can produce a biphasic response in its ability to alter the firing of APs. A lower concentration (1 μM) of ranolazine increased AP firing, while the firing rate was reduced at a higher concentration (10 μM) compared to the low concentration.

Materials and Methods

Cell preparations

Rat pituitary GH_3 cells, obtained from the Bioresources Collection and Research Center (BCRC-60015; Hsinchu, Taiwan), were maintained in Ham's F-12 medium (Life Technologies, Carlsbad, CA, USA) supplemented with 15% horse serum, 2.5% fetal calf serum, and 2 mM L-glutamine in a humidified environment of 5% CO_2 / 95% air (20). In order to promote differentiation, cells were transferred to a serum- and Ca^{2+}-free medium. Under these conditions, cells remained 80% – 90% viable for at least two weeks.

Human embryonic kidney (HEK293T) cells were obtained from the American Type Culture Collection (CRL-11268; Manassas, VA, USA). They were maintained in Dulbecco's modified Eagle's medium (DMEM) (Life Technologies) supplemented with 10% heat-inactivated fetal bovine serum, 2 mM L-glutamine, 100 units/ml penicillin, and 100 μg/ml streptomycin at 37°C in a 5% CO_2 atmosphere. For transfection of HEK293T cells, $2 – 6 \times 10^4$ cells were seeded in each well of a 24-well culture plate for 24 h.

The clonal strain NG108-15 cell line was obtained from the European Collection of Cell Cultures (ECACC-88112302; Wiltshire, UK). Cells were grown in monolayer cultures in plastic disks containing DMEM supplemented with 100 μM hypoxanthine, 1 μM aminopterin, 16 μM thymidine, and 5% fetal bovine serum as the culture medium, in a humidified incubator equilibrated at 37°C in a 5% CO_2 atmosphere (20). To induce neuronal differentiation, culture medium was replaced with medium containing 1 mM dibutyryl cyclic-AMP and cells were cultured in the incubator for 1 – 7 days.

Transfection

The expression vector pCMV6-XL4 containing a human voltage-dependent and Ca^{2+}-activated K^+ channel pore-forming α-subunit (*α-hSlo*; NM_002247.1) was purchased from Origene Technologies (Rockville, MD, USA). The *α-hSlo* gene is known to encode a functional large-conductance Ca^{2+}-activated K^+ (BK_{Ca}) channel. The expression plasmid was transfected into HEK293T cells for transient expression. The plasmid was prepared in 150 mM NaCl as a diluent solution. Polyethylenimine (PEI) (MBI Fermentas, Hanover, MD, USA) and plasmid were mixed together and incubated for 10 min at room temperature for adequate binding of the plasmid to the PEI. Plasmid-PEI mixture solution was added to the 24-well plate and centrifuged at 280 × *g* for 5 min. Subsequently, transfected cells were incubated at 37°C for an additional 48 h.

Electrophysiological measurements

Before the experiments, cells were dissociated with 1% trypsin/EDTA solution and an aliquot of cell suspension was transferred to a recording chamber affixed to the stage of a DM-IL inverted microscope (Leica, Wetzlar, Germany). Cells were bathed at room temperature (20°C – 25°C) in normal Tyrode's solution containing 1.8 mM $CaCl_2$. Microelectrodes were pulled from Kmax-51 capillaries (Kimble Glass, Vineland, NJ, USA) using a PP-830 puller (Narishige, Tokyo), and had a resistance of 3 – 5 MΩ when filled with different intracellular solutions. Patch clamp recordings were obtained in cell-attached, inside-out, or whole-cell configurations using an RK-400 amplifier (Bio-Logic, Claix, France) (14).

Data recordings

The signals were displayed with a digital oscilloscope (model 1602; Gould, Chandler, AZ, USA). The data were stored online in a Slimnote V x 3 computer (Lemel, Taipei, Taiwan) equipped with a Digidata 1322A interface (Molecular Devices), which was controlled by pCLAMP 9.0 (Molecular Devices). Currents were low pass-filtered at 3 kHz. The pCLAMP-generated voltage-step protocols were employed to determine current–

voltage (*I–V*) relationships for ion currents. Ion currents recorded during whole-cell or single-channel experiments were analyzed by using Origin 7.5 (OriginLab, Northampton, MA, USA) or custom-made macros built in an Excel 2007 spreadsheet running on Windows Vista (Microsoft, Redmond, WA, USA).

Data analyses

To calculate percentage inhibition of ranolazine on I_{Na}, the current amplitudes during the application of ranolazine were compared with those measured after a subsequent application of tetrodotoxin (1 μM). The concentration-dependent relation of ranolazine on the inhibition of $I_{K(IR)}$ or I_{Na} was fitted to the Hill equation:

$$\text{percentage inhibition} = \frac{E_{max} \times [\text{drug}]^{n_H}}{IC_{50} + [\text{drug}]^{n_H}}$$

, where [drug] represents the concentration of ranolazine; IC_{50} and n_H are the concentration required for a 50% inhibition and the Hill coefficient, respectively; and E_{max} is the ranolazine-induced maximal inhibition of $I_{K(IR)}$ (i.e., E-4031–sensitve current) or I_{Na} (i.e., tetrodotoxin-sensitive current).

To examine the effect of ranolazine on the steady-state activation curve of $I_{K(IR)}$, the relationships between the conditioning pulses and the normalized amplitudes of $I_{K(IR)}$ with or without application of ranolazine (1 μM) were constructed and fitted by the Boltzmann equation:

$$I = \frac{I_{max}}{1 + \exp\left(\frac{(V - V_{1/2})qF}{RT}\right)}$$

, where I_{max} is the maximal activated $I_{K(IR)}$;V, the membrane potential in mV; $V_{1/2}$, the membrane potential for a half-maximal activation; q, the gating charge; F, the Faraday's constant; R, the universal gas constant; and T, the absolute temperature.

The frequency of spontaneous APs was characterized by transforming the oscillating signals from their time domain to their representation in the frequency domain with the aid of power spectral analysis (14). Spectral analyses were performed using a discrete Fourier transform algorithm by using Origin 7.5 (OriginLab). When the firing of APs displayed a regular discharge pattern, the mean firing frequency would fall in a concentrated peak in the power spectrogram.

All values are given as means ± S.E.M. with sample sizes (n) indicating the number of cells examined, and error bars are plotted as S.E.M. The paired or unpaired Student's *t*-test and one-way ANOVA with the least-significance-difference method for multiple comparisons were used for the statistical evaluation of differences among the mean values. Differences between the values were considered significant at a value of $P<0.05$.

Drugs and solutions

Ranolazine hydrochloride (RS-43285; Ranexa®; $C_{24}H_{33}N_3O_4$; (±)-*N*-(2,6-dimethyl-phenyl)-4[2-hydroxy-3(2-methoxy-phenoxy)propyl]-1-piperazine acetamide) and riluzole were obtained from Tocris Cookson, Ltd. (Bristol, UK), Tetraethylammonium chloride was from Sigma-Aldrich (St. Louis, MO, USA), tetrodotoxin was from Alomone Labs (Jerusalem, Israel), and Bay K 8644, dibutyryl cyclic AMP and E-4031 were from Biomol (Plymouth Meeting, PA, USA). Fisetin was obtained from the Pharmaceutical Industry Technology and Development Center (Taipei, Taiwan). Ranolazine was prepared as 1 – 10 mM stock solutions in distilled water.

The composition of the bath solution (i.e., normal Tyrode's solution) was 136.5 mM NaCl, 5.4 mM KCl, 1.8 mM $CaCl_2$, 0.53 mM $MgCl_2$, 5.5 mM glucose, and 5.5 mM HEPES-NaOH buffer, pH 7.4. To record $I_{K(DR)}$ or membrane potential, patch pipettes were filled with a solution consisting of 140 mM KCl, 1 mM $MgCl_2$, 3 mM Na_2ATP, 0.1 mM Na_2GTP, 0.1 mM EGTA, and 5 mM HEPES-KOH buffer, pH 7.2. To measure $I_{K(IR)}$, bath solution was replaced with a high-K^+, Ca^{2+}-free solution containing 130 mM KCl, 10 mM NaCl, 3 mM $MgCl_2$, 6 mM glucose, and 10 mM HEPES-KOH, pH 7.4. To record I_{Na} or $I_{Ca,L}$, KCl inside the pipette solution was replaced with equimolar CsCl, and pH was adjusted to 7.2 with CsOH. For single-channel recordings on HEK293T cells, high K^+-bathing solution contained 145 mM KCl, 0.53 mM $MgCl_2$, and 5 mM HEPES-KOH, pH 7.4; and the pipette solution contained 145 mM KCl, 2 mM $MgCl_2$, and 5 mM HEPES-KOH, pH 7.2. The value of free Ca^{2+} concentration was calculated assuming a dissociation constant for EGTA and Ca^{2+} (at pH 7.2) of 0.1 μM. To provide 0.1 μM Ca^{2+} in the bath solution for measurement of the BK_{Ca} channel, 0.5 mM $CaCl_2$ and 1 mM EGTA were added.

Results

Inhibitory effect of ranolazine on I_{Na} in pituitary GH_3 cells

In the initial set of experiments, a whole-cell configuration was used to investigate the effect of ranolazine on macroscopic ion currents in GH_3 cells. Cells were bathed in Ca^{2+}-free Tyrode's solution containing 10 mM tetraethylammonium chloride and patch pipettes were loaded with a Cs^+-containing solution. When the depolarizing pulses from −80 to different membrane

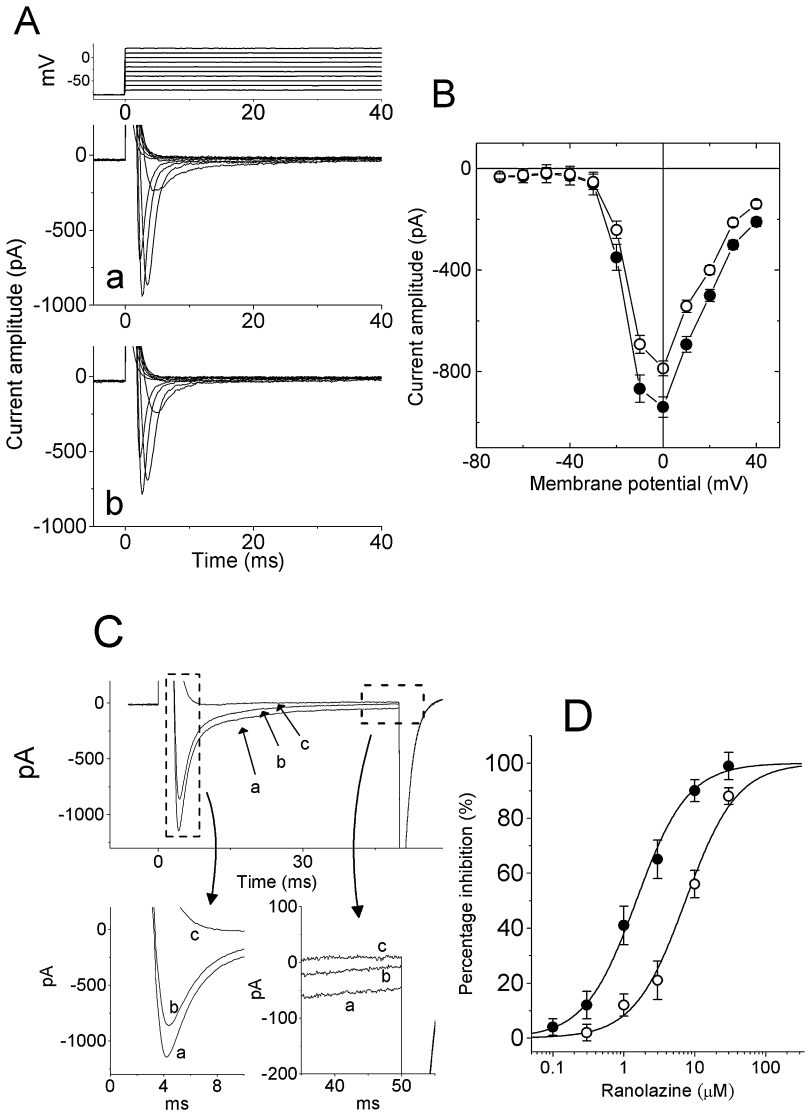

Fig. 1. Inhibitory effects of ranolazine on I_{Na} in GH_3 cells. In these experiments, each pipette was loaded with a Cs^+-containing solution, and cells were bathed in Ca^{2+}-free Tyrode's solution containing 10 mM tetraethylammonium chloride. The cell was depolarized from −80 mV to different membrane potentials with a duration of 100 ms at a rate of 0.1 Hz. A: Superimposed traces of I_{Na} obtained in the absence (a) or presence (b) of 1 μM ranolazine. The uppermost portion shown in this and the following figures generally indicates the voltage protocol used. B: Averaged *I–V* relationships of transient and late I_{Na} obtained in control (filled circles) and during the exposure to ranolazine (open circles). Each point represents the mean ± S.E.M. (n = 6 – 8). C: Concentration-dependent inhibition of I_{Na} by ranolazine in GH_3 cells. In these experiments, each cell was depolarized from −80 to −20 mV with a duration of 50 ms. Original current traces obtained in the control and during exposure to ranolazine and ranolazine plus tetrodotoxin. Trace a is the control, trace b was recorded in the presence of 3 μM ranolazine, and trace c was recorded after further application of tetrodotoxin (1 μM), but in the continued presence of ranolazine (3 μM). The lower portions in panel C indicate expanded records from upper portion (dashed box). D: Concentration–response relationships for ranolazine-induced inhibition of I_{Na} (i.e., tetrodotoxin-sensitive current) measured at the beginning (open circles) and end (filled circles) of depolarizing pulses (mean ± S.E.M., n = 5 – 10 for each point). Smooth lines represent the best fits to the Hill equation as described in Materials and Methods. Notably, in order to compare the effects of ranolazine on the peak and late I_{Na}, we selected the cells showing larger peak I_{Na}.

potentials were applied to evoke I_{Na}, application of ranolazine (1 μM) decreased the peak amplitude of I_{Na}, together with an increase in current inactivation (Fig. 1A). This inhibitory effect was readily reversed on washout of this drug. Figure 1B illustrates the *I–V* relationships of I_{Na} measured at the beginning of the depolarizing pulses in the control and during the exposure to ranolazine (1 μM). No change in the configuration of the overall *I–V* relationship of I_{Na} was seen in the presence of ranolazine (1 μM). However, the magnitude of ranolazine-mediated inhibition of I_{Na} measured at the beginning and end of the depolarizing pulses was found to be different. The relationships between the concentration of ranolazine and the percentage inhibition for transient and late components of I_{Na} are illustrated in Fig. 1, C and D. The IC_{50} values required for the inhibitory effects of ranolazine on transient and late components of I_{Na} were 7.4 and 1.5 μM, respectively. Therefore, the data showed that consistent with previous observations made in heart cells (2, 3), during exposure to this drug, the late component of I_{Na} was inhibited to a greater extent than the transient component of I_{Na}.

Lack of effect of ranolazine on $I_{Ca,L}$ in pituitary GH_3 cells

Because this drug was previously reported to suppress the amplitude of $I_{Ca,L}$ in heart cells (19, 21, 22), we addressed the issue of whether ranolazine exerts any effects on this current in these cells. To answer this question, the experiments were conducted in GH_3 cells bathed in normal Tyrode's solution containing 1.8 mM $CaCl_2$ and 1 μM tetrodotoxin. As shown in Fig. 2, the peak amplitudes of $I_{Ca,L}$ obtained after application of ranolazine at a concentration of 30 μM did not differ significantly from those in the control condition. However, a subsequent application of fisetin, a flavonoid

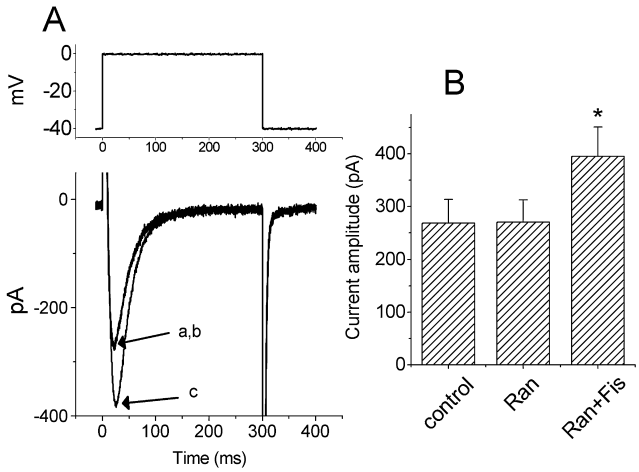

Fig. 2. Lack of effect of ranolazine on $I_{Ca,L}$ in GH_3 cells. Similar to the experiments made for the recordings of I_{Na}, patch pipettes were loaded with a Cs^+-containing solution. However, cells were bathed in normal Tyrode's solution that contained 1.8 mM $CaCl_2$, 10 mM tetraethylammonium chloride, and 1 μM tetrodotoxin. A: Superimposed current traces obtained when the cell was depolarized from −40 to 0 mV at a rate of 0.1 Hz. Trace a is the control, trace b was obtained in the presence of ranolazine (30 μM), and trace c was obtained after further addition of fisetin (10 μM), but still in the presence of ranolazine (30 μM). B: Bar graph showing the effects of ranolazine and ranolazine plus fisetin on the peak amplitude of $I_{Ca,L}$ in GH_3 cells (mean ± S.E.M., n = 5 – 8 for each bar). In the experiments with ranolazine plus fisetin, fisetin (10 μM) was applied after addition of ranolazine (30 μM). Ran: 30 μM ranolazine, Fis: 10 μM fisetin. *P<0.05, significantly different from the control. Note that ranolazine exerts little or no effect on $I_{Ca,L}$.

known to open L-type Ca^{2+} channels (23), could increase the peak amplitude of $I_{Ca,L}$ significantly. Similarly, in the continued presence of ranolazine (30 μM), further application of Bay K 8644 (10 μM) was also effective in increasing $I_{Ca,L}$ (data not shown). Therefore, the results indicate that unlike I_{Na}, $I_{Ca,L}$ present in GH_3 cells tends to be refractory to inhibition by this drug.

Effect of ranolazine on $I_{K(IR)}$ in pituitary GH_3 cells

Earlier work has demonstrated that ranolazine is able to block the *HERG* K^+ current expressed in *Xenopus* oocytes and HEK293 cells (18, 19). It would thus be essential to evaluate if there are any effects of this drug on $I_{K(IR)}$ in GH_3 cells. In these experiments, when cells were bathed in a high-K^+, Ca^{2+}-free solution, a family of large inward currents (i.e., $I_{K(IR)}$) could be elicited upon membrane hyperpolarizations (14, 24). During membrane hyperpolarization, there was an instantaneous current followed by a voltage- and time-dependent elicitation of K^+ inward current (i.e., deactivating tail K^+ current). These inward currents decayed at potential below −50 mV and current deactivation became faster with greater hyperpolarizations. When cells were exposed to ranolazine (1 μM), the amplitude of $I_{K(IR)}$ was greatly reduced (Fig. 3). For example, when cells were hyperpolarized from −10 to −120 mV, ranolazine (1 μM) significantly decreased the amplitude of peak inward currents by 49 ± 7% from 781 ± 31 to 396 ± 29 pA (P<0.05, n = 9). After washout of drug, current amplitude was partially returned to the control level. Figure 3B illustrates the *I–V* relationships of $I_{K(IR)}$ obtained at the beginning and end of the hyperpolarizing

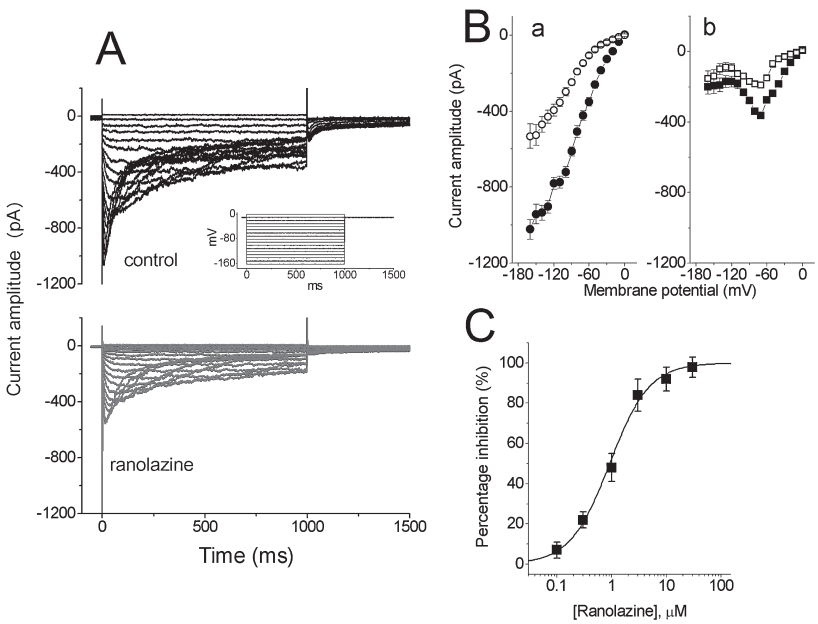

Fig. 3. Inhibitory effect of ranolazine on the *I–V* relationships of the hyperpolarization-evoked current in pituitary GH_3 cells. Cells were bathed in a high-K^+, Ca^{2+}-free solution containing tetrodotoxin (1 μM) and $CdCl_2$ (0.5 mM). A: Superimposed current traces obtained when a cell was held at −10 mV and different voltage pulses ranging from 0 to −160 mV were applied. Current traces shown in upper portion are controls and those in lower portion were obtained after application of ranolazine (1 μM). The inset indicates the voltage protocol used. B: Averaged *I–V* relationships of $I_{K(IR)}$ in the absence (filled symbols) and presence (open symbols) of 1 μM ranolazine. The results shown in Ba and Bb were, respectively, obtained at the beginning and end of the voltage pulses (mean ± S.E.M., n = 9 – 12 for each point). C: Concentration–response relationship for ranolazine-induced inhibition of $I_{K(IR)}$ (i.e., E-4031–sensitive current). Each point represents the mean ± S.E.M. (n = 6 – 11). The smooth line represents the best fit to the Hill equation. The values for IC_{50}, maximally inhibited percentage of E-4031–sensitive current, and Hill coefficient were 0.92 μM, 100% and 1.2, respectively.

pulses. During cell exposure to ranolazine (1 μM), the slope of the linear fit of the current amplitude to the voltages between −120 and −60 mV was significantly reduced from 6.9 ± 0.2 to 4.6 ± 0.1 nS (P<0.05, n = 8).

The relationship between the concentration of ranolazine and the percentage inhibition of $I_{K(IR)}$ is illustrated in Fig. 3C. To evoke $I_{K(IR)}$, each cell was hyperpolarized from −10 to −120 mV. The peak amplitudes of $I_{K(IR)}$ in the presence of ranolazine were compared with those obtained after subsequent application of E-4031 (10 μM). Addition of ranolazine (0.1 – 30 μM) was noted to suppress the amplitudes of E-4031–sensitive currents in a concentration-dependent manner. The half-maximal concentration (i.e., IC_{50}) required for inhibitory effect of ranolazine on $I_{K(IR)}$ was 0.92 μM, and this drug at a concentration of 30 μM nearly abolished the amplitude of $I_{K(IR)}$.

Effect of ranolazine on the steady-state activation of $I_{K(IR)}$ in GH_3 cells

To further characterize the inhibitory effect of ranolazine on $I_{K(IR)}$, we next investigated whether this drug modifies the steady-state activation of $I_{K(IR)}$. A two-step voltage protocol was applied in these experiments (Fig. 4A). In this set of experiments, a 1-s conditioning pulse to different membrane potentials preceded a test potential (300 ms in duration) to −110 mV from a holding potential of −10 mV. The relationships between the conditioning pulses and the normalized amplitudes of $I_{K(IR)}$ were then constructed and fitted by the Boltzmann distribution as described in Materials and Methods. Figure 4B illustrates the steady-state activation curve of $I_{K(IR)}$ in the absence and presence of ranolazine. In the control, $V_{1/2} = -93.8 \pm 1.1$ mV, $q = 3.5 \pm 0.1$ e (n = 8), whereas, during exposure to ranolazine (1 μM), $V_{1/2} = -82.7 \pm 0.9$ mV, $q = 3.4 \pm 0.1$ e (n = 8). Notably, not only did ranolazine decrease the amplitude of $I_{K(IR)}$, but it also produced an approximately 11-mV right shift in the activation curve of this current. However, the gating charge (i.e., q) of the *erg* channel did not differ significantly between the absence and presence of 1 μM ranolazine (P>0.05, n = 8). These results indicate that in GH_3 cells, this drug can shift the voltage-dependence of $I_{K(IR)}$ with no apparent change in the gating charge of the channel.

Effect of ranolazine on the deactivation of $I_{K(IR)}$ in GH_3 cells

Deactivation kinetics with or without addition of ranolazine were further evaluated. In these experiments, the test pulses were preceded by a fixed, highly hyperpolarized prepulse (−130 mV for 30 ms) that would activate virtually all channels and uncouple the activation process from block. Following the prepulse, a range of voltage pulses between −140 and −90 mV was delivered. The rate of current decay (i.e., $1/\tau$) upon stepping to the different voltages was then measured. Figure 5A illustrates superimposed current traces obtained in the absence and presence of 3 μM ranolazine. The current decays were fitted with a single exponential and their reciprocal time constants ($1/\tau$) were then constructed and plotted against the test potentials (Fig. 5B). The data suggest that ranolazine can reduce the deactivation rate of $I_{K(IR)}$ at every voltage measured. The difference in the value of $1/\tau$ between the absence and presence of ranolazine tends to be greater with more hyperpolarization.

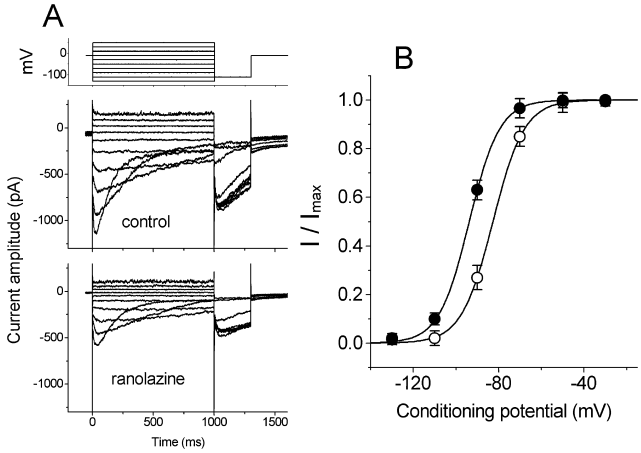

Fig. 4. Effects of ranolazine on the steady-state activation curve of $I_{K(IR)}$ in GH_3 cells. By use of a two-step protocol, the steady-state activation parameters of $I_{K(IR)}$ were obtained with or without application of ranolazine (1 μM). The conditioning voltage pulses with a duration of 1 s for different membrane potentials were applied from a holding potential of −10 mV. After each conditioning pulse, a test pulse to −110 mV with a duration of 300 ms was applied to evoke $I_{K(IR)}$. A: Superimposed current traces obtained when the cell was hyperpolarized from a holding potential −10 to −110 mV with different conditioning potentials. The records shown in upper portion are controls, and those in the lower portion were obtained 1 min after addition of ranolazine (1 μM). B: Steady-state activation curve of $I_{K(IR)}$ in the absence (filled circles) and presence (open circles) of 1 μM ranolazine (mean ± S.E.M., n = 5 – 9 for each point). Smooth lines represent the best fits to the Boltzmann equation as described in Materials and Methods. Notably, when cells were exposed to ranolazine, the voltage for half-maximal activation of $I_{K(IR)}$ was shifted to a rightward direction by +11 mV.

Inhibitory effect of ranolazine on $I_{K(DR)}$ in GH_3 cells

We next determined the ability of ranolazine to affect the amplitude of $I_{K(DR)}$ that is present in these cells. In these experiments, cells were bathed in Ca^{2+}-free, Tyrode's solution containing 1 μM tetrodotoxin and 0.5 mM $CdCl_3$. Each cell was held at −50 mV and different potentials ranging from −50 to +40 mV in 10-mV increments were applied. As shown in Fig. 6,

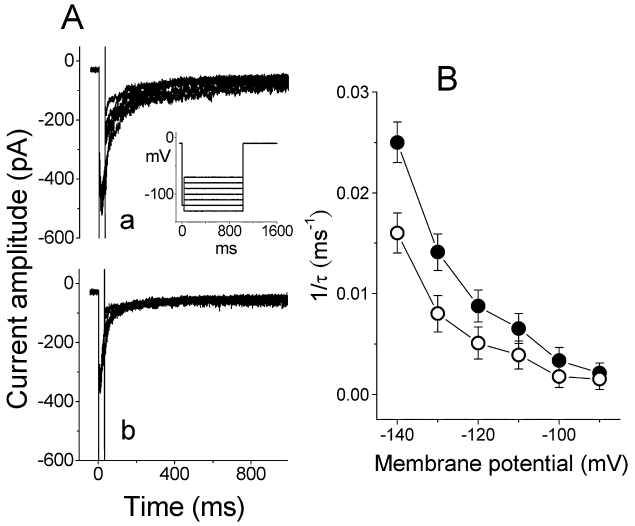

Fig. 5. Effect of ranolazine on $I_{K(IR)}$ deactivation in GH_3 cells. Cells were bathed in a high-K^+, Ca^{2+}-free solution. The conditioning pulses were hyperpolarized from −10 to −130 mV with a duration of 30 ms. After each conditioning pulse, different membrane potentials ranging from −140 to −90 mV in 10-mV increments were applied. A: Superimposed current traces obtained in the absence (a) and presence (b) of 3 μM ranolazine. The inset indicates the voltage protocol used. In panel B, the reciprocal of the time constant obtained by single-exponential fit of each current decay in the absence (filled circles) and presence (open circles) of 3 μM ranolazine was plotted against the membrane potential (mean ± S.E.M., n = 6 – 8 for each point).

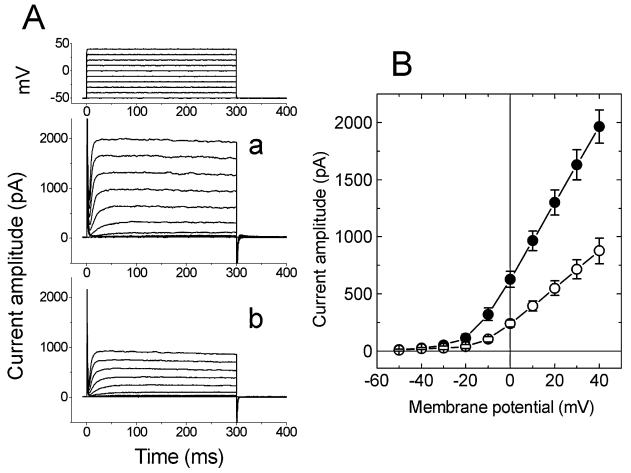

Fig. 6. Inhibitory effect of ranolazine on $I_{K(DR)}$ in GH_3 cells. In these experiments, cells, bathed in a Ca^{2+}-free Tyrode's solution contained tetrodotoxin (1 μM) and $CdCl_2$ (0.5 mM), were held at −50 mV, and the depolarizing pulses from −50 to +40 mV in 10-mV increments were applied at a rate of 0.05 Hz. A: Superimposed current traces shown in the upper portion (a) are the control, and those in the lower portion (b) are the results obtained 2-min after application of ranolazine (30 μM). B: Averaged *I–V* relationships of $I_{K(DR)}$ in the control (filled circles) and during exposure to 30 μM ranolazine (open circles) (mean ± S.E.M., n = 6 – 9 for each point).

addition of ranolazine at a concentration of 30 μM depressed the amplitude of $I_{K(DR)}$ over the entire range of test potentials. For example, ranolazine (10 μM) decreased current amplitude at the level of +40 mV by 28 ± 3% (P<0.05, n = 7); and at the same level of holding potential, ranolazine (30 μM) reduced current amplitude by 52 ± 3% (n = 7) from 1963 ± 145 to 876 ± 112 pA (P<0.05, n = 7). Thus, it is clear that, as compared with $I_{K(IR)}$, $I_{K(DR)}$ present in GH_3 cells is relatively unresponsive to inhibition by ranolazine.

Effects of ranolazine on $I_{K(Ca)}$ in GH_3 cells

Some of agents known to block I_{Na} (e.g., riluzole and vinpocetine) were noted to activate $I_{K(Ca)}$ (8, 9). It was thus investigated whether ranolazine has any effect on $I_{K(Ca)}$ in these cells. When cells were exposed to ranolazine at a concentration less than 10 μM, no change in the amplitude of $I_{K(Ca)}$ could be demonstrated. However, application of ranolazine at 30 μM reduced the amplitude of $I_{K(Ca)}$ throughout the entire voltage-clamp step (Fig. 7). Distinguished from the actions of riluzole or vinpocetine, the inhibitory effect on $I_{K(Ca)}$ caused by ranolazine at high concentrations (≥30 μM) can be observed. $I_{K(Ca)}$ is relatively less sensitive to block by ranolazine than $I_{K(DR)}$.

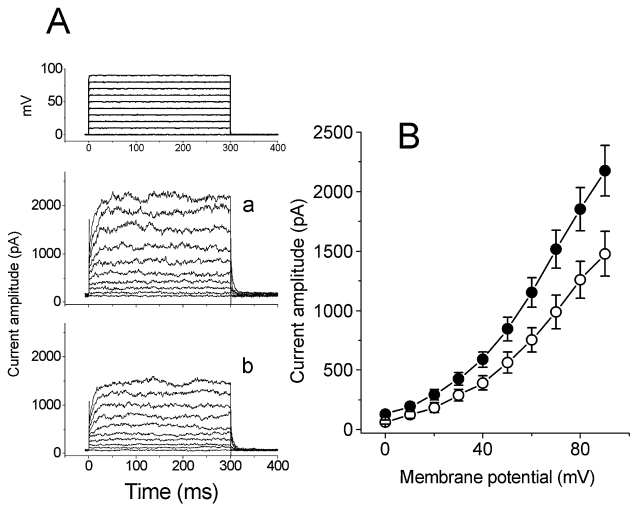

Fig. 7. Inhibitory effect of ranolazine on $I_{K(Ca)}$ in GH_3 cells. A: Superimposed current traces in the control (a) and during exposure to 30 μM ranolazine (b). In these experiments, cells were bathed in normal Tyrode's solution containing 1.8 mM $CaCl_2$. The cell was held at 0 mV and the voltage pulses from 0 to +90 mV in 10-mV increments with a duration of 300 ms were delivered. B: Averaged *I–V* relationships of $I_{K(Ca)}$ in the control (filled circles) and during exposure to 30 μM ranolazine (open circles) (mean ± S.E.M., n = 7 – 10 for each point).

Inhibitory effect of ranolazine on the α-hSlo channel expressed in HEK293T cells

In a separate set of experiments, we also tested the

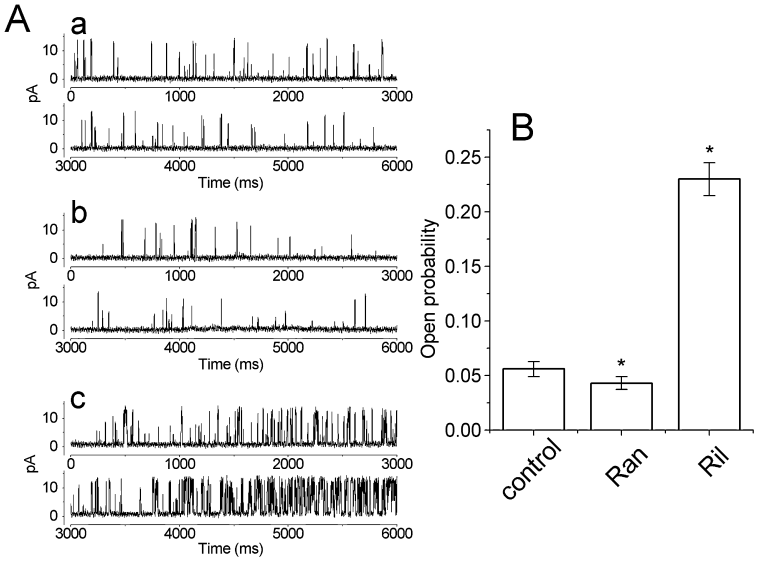

Fig. 8. Effects of ranolazine and riluzole on BK_{Ca}-channel activity recorded from *α-hSlo*–expressing HEK293T cells. A: Original current traces showing the channel activity in the control (a) and in the presence of 30 μM ranolazine (b) or 10 μM riluzole (c). Inside-out recordings were conducted with a symmetrical K^+ solution (145 mM). The potential was constantly held at +60 mV, and the bath medium contained 0.1 μM Ca^{2+}. B: Summary of data showing the effects of ranolazine and riluzole on BK_{Ca}-channel activity in *α-hSlo*–expressing HEKT293T cells (mean ± S.E.M., n = 5 – 8 for each bar). Ran: ranolazine (30 μM), Ril: riluzole (10 μM). **P*<0.05, significantly different from the control.

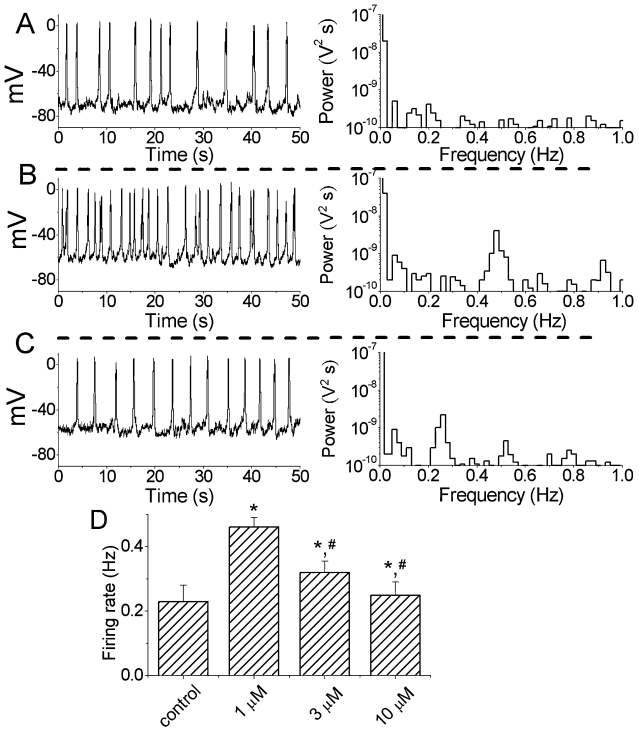

Fig. 9. Biphasic effect of ranolazine on spontaneous APs in GH_3 cells. Cells were bathed in normal Tyrode's solution containing 1.8 mM $CaCl_2$. These experiments were performed under current-clamp conditions. The left and right sides shown in each panel, respectively, indicate potential traces and spectral patterns of corresponding APs. Panel A is the control, and panels B and C are the results obtained in the presence of 1 and 10 μM ranolazine, respectively. Notably, when cells were exposed to ranolazine, the repetitive firing was converted from an irregular (A) to a regular pattern [(B) and (C)]. D: Summary of data depicting effects of ranolazine (1, 3, and 10 μM) on the firing frequency of APs (mean ± S.E.M., n = 8 – 10 for each bar). **P*<0.05, significantly different from the control. $^{\#}P$<0.05, significantly different from the ranolazine (1 μM)-alone group.

hypothesis that ranolazine exerts effects on the activity of BK_{Ca} channels in HEK293T cells transfected with *α-hSlo*. Under our experimental conditions, the transfection of *α-hSlo* in HEK293T cells could result in the appearance of BK_{Ca} channels (25). In the inside-out configuration, when ranolazine (30 μM) was applied to the intracellular side of the excised patch, BK_{Ca}-channel activity in *α-hSlo*–expressing HEK293T cells was reduced (Fig. 8). However, no discernible change in single-channel conductance was seen in the presence of ranolazine. Alternatively, riluzole (10 μM), known to block persistent Na^+ channels and to stimulate BK_{Ca} channels (8), was capable of enhancing channel activity in these cells. These results showed that, compatible with the results on the measurement of $I_{K(Ca)}$ in GH_3 cells, ranolazine could reduce the probability of channel openings in HEK293T cells expressing *α-hSlo*. The BK_{Ca}-channel α-subunit is thus a likely target for the action of this drug, if the concentrations used are greater than 30 μM.

Effect of ranolazine on the firing of APs

To determine the ability of ranolazine to produce any change in the membrane potential of GH_3 cells, the final set of experiments were conducted with K^+-containing pipette solution with cells bathed in normal Tyrode's solution containing 1.8 mM $CaCl_2$, and current-clamp recordings were made. Figure 9 illustrates the effect of ranolazine on the AP firing in GH_3 cells. When this drug at concentrations below 3 μM was applied to the cells, the firing rate of APs was progressively increased. When cells were exposed to ranolazine (1 μM), the membrane potential was depolarized to −61 ± 5 mV (n = 7) from a control value of −66 ± 5 mV (*P*<0.05, n = 9). As shown

in Fig. 9D, ranolazine (1 μM) significantly increased the firing rate of APs; however, ranolazine at a concentration of 10 μM resulted in a reduction in AP firing. The firing rate of APs during the exposure to 10 μM ranolazine was reduced.

The effect of ranolazine on the firing pattern of APs was further characterized. To analyze the discharge pattern of spontaneous APs, power spectral analyses of the changes in membrane potential that can convert the time domain to the frequency domain were made (14). As shown in Fig. 9, the majority of GH_3 cells in the control condition exhibited a scattered power density in the spectrogram which indicated that an irregular pattern of repetitive firing was seen in these cells. However, when cells were exposed to ranolazine (1 μM), the discharge pattern of these cells exhibited a concentrated peak at approximately 0.48 Hz with subsequent harmonic components appearing at multiples of 0.48 Hz, for example, 0.92 Hz. Similar results were obtained in seven different cells. Furthermore, further application of ranolazine (10 μM) reduced the firing rate of APs, thereby producing a concentrated peak at approximately 0.25 Hz that indicates a regular pattern of AP firing. Therefore, the results indicate that exposure of GH_3 cells to ranolazine is able to produce a biphasic action on AP firing. The stimulatory effect on AP firing caused by ranolazine at lower concentrations is associated with the inhibition of $I_{K(IR)}$, while during the exposure to this drug at higher concentrations, the inhibitory effect on the spontaneous discharge emerges owing primarily to its inhibition of I_{Na}.

Effect of ranolazine on I_{Na} and $I_{K(IR)}$ in NG108-15 neuronal cells

Finally, to verify whether the ranolazine-induced inhibition of I_{Na} and $I_{K(IR)}$ could be observed in neurons, we also determined the ability of this drug to modify these two types of ion currents in NG108-15 neuronal cells. As shown in Fig. 10, this drug significantly diminished the amplitudes of both I_{Na} and $I_{K(IR)}$ in a concentration-dependent manner. For example, ranolazine (3 μM) decreased I_{Na} from 2084 ± 25 to 1649 ± 18 pA (P<0.05, n = 7), while this drug at the same concentration decreased $I_{K(IR)}$ from 1684 ± 27 to 945 ± 20 pA (P<0.05, n=7). Therefore, similar to the results obtained in GH_3 cells, the block of $I_{K(IR)}$ by ranolazine tends to be more potent than that of I_{Na} measured at the beginning of the voltage pulse (i.e., transient I_{Na}).

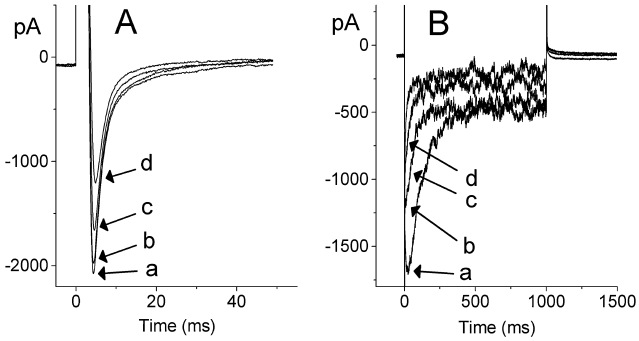

Fig. 10. Effect of ranolazine on I_{Na} and $I_{K(IR)}$ in NG108-15 neuronal cells. A: Superimposed I_{Na} evoked from −80 to −10 mV with a duration of 50 ms. The patch pipette was filled with Cs^+-containing solution, and NG108-15 cells were bathed in Ca^{2+}-free Tyrode's solution containing 10 mM tetraethylammonium chloride. B: Superimposed $I_{K(IR)}$ evoked from −10 to −120 mV with a duration of 1 s. Cells were bathed in high-K^+, Ca^{2+}-free solution and the patch pipette was filled with K^+-containing solution. In panels A and B, trace a is the control, and traces b, c, and d are, respectively, obtained after the addition of 1, 3, and 10 μM ranolazine.

Discussion

The major findings of this study are as follows: First, in pituitary GH_3 cells, ranolazine, a piperazine derivative, differentially inhibited the transient and late components of I_{Na} in a concentration-dependent manner; however, it had no effects on $I_{Ca,L}$. Second, ranolazine was effective in suppressing the amplitude of $I_{K(IR)}$. Third, this drug can modify the activation and deactivation kinetics of $I_{K(IR)}$. Fourth, at a high concentration, it could reduce the amplitude of $I_{K(DR)}$ and $I_{K(Ca)}$ and the activity of BK_{Ca} channels. Fifth, it exerted a biphasic action on the firing of spontaneous APs. Sixth, ranolazine blocked I_{Na} and $I_{K(IR)}$ in NG108-15 neuronal cells. Taken together, these results suggest that the inhibition by ranolazine of these ion channels can be one of ionic mechanisms underlying its changes in the functional activities of neurons and endocrine or neuroendocrine cells, assuming that similar results can be found in vivo.

Previous reports have demonstrated that ranolazine could preserve intracellular ATP content in heart cells during the ischemic state via its reduction of fatty-acid β-oxidation (26 – 28). In our whole-cell experiments, the recording pipettes constantly contained 3 mM ATP. In GH_3 cells loaded with the pipette solution containing no ATP, ranolazine-mediated inhibition of I_{Na} or $I_{K(IR)}$ remained unaltered. The inhibitory effect of this drug was also found to be rapidly developing and readily washed out. The concentration of ranolazine required for the inhibition of $I_{K(IR)}$ or I_{Na} is lower than that for the inhibition of fatty acid oxidase (26). The observed effect of ranolazine on these ion currents is thus unlinked to its inhibitory effect on β-oxidation of fatty acids and can be due to the drug acting on the channel itself.

The IC_{50} value of ranolazine required for the inhibition of $I_{K(IR)}$ in GH_3 cells was approximately 0.92 μM

in this study. This value is greater than those for the ranolazine-induced block of *HERG* channel expressed in *Xenopus* oocytes (19) and HEK293 cells (18). This discrepancy remains to be determined. However, it should be noted that the studies based on the usefulness of HERG current are limited owing to the non-native conditions (e.g., α-subunits) of the ion channel in *Xenopus* oocytes or in the host HEK293 cells. Moreover, GH_3 cells used in this study were reported to contain many different isoforms of endogenous *erg* channels (10, 13). The issues of whether other isoforms of *erg* channels are subject to more sensitive to block by ranolazine remain to be clarified. Other auxiliary subunits of the *erg* channels may potentiate its inhibitory effect on $I_{K(IR)}$. Nevertheless, the IC_{50} values for ranolazine-mediated inhibition of $I_{K(IR)}$ and late component of I_{Na} is lower than therapeutic plasma concentrations ($2-6\,\mu$M). Because ranolazine can affect β-oxidation of fatty acids inside the cell, the cell membrane is likely to be permeable to the ranolazine molecule. It still remains to be clarified whether ranolazine can effectively pass through blood-brain barrier to reach neurons. Moreover, the protein binding of this compound (about 61% – 64%) may hinder it from entering the nervous system (29). Nevertheless, block of $I_{K(IR)}$ in cells like neurons and endocrine or neuroendocrine cells may thus be a relevant target for the action of this drug.

In our study, the presence of ranolazine not only reduced the maximal conductance of $I_{K(IR)}$ but produced a positive shift in the steady-state activation curve as well. The lack of any change in the slope factor of the activation curve of $I_{K(IR)}$ during exposure to this agent suggests that the interaction with the *erg* channels is not mediated by a direct effect on the voltage sensor *per se* and that its binding site may lie outside of the transmembrane field. An important functional consequence of a rightward shift of the activation curve is an increased excitability at voltages near the resting potential, along with enhanced spike activity in these cells. Reduction of deactivating $I_{K(IR)}$ accompanied by the rightward shift of the activation curve also suggests a relative decrease in open state stability of the channel during the exposure to ranolazine. As a result, the sensitivity to ranolazine in neurons and endocrine or neuroendocrine cells would rely on the preexisting level of resting potential, the AP firing, or the concentration of ranolazine used.

The IC_{50} value of ranolazine required for the inhibition of late I_{Na} was 1.5 μM. This value tends to be higher than that for its inhibitory effect on $I_{K(IR)}$. One would expect that the increase of AP firing caused by ranolazine at lower concentrations may be opposed by its inhibition of late I_{Na}. However, through an inhibition of $I_{K(IR)}$, it may depolarize the cell and exacerbate the inhibition of I_{Na} to a greater extent, thereby diminishing its depressant action on late I_{Na}. The reduction of AP firing caused by ranolazine at concentrations greater than 10 μM could be explained by its ability to inhibit the transient and late components of I_{Na} in pituitary GH_3 cells. Nevertheless, the results from our studies imply that block of *erg* channels by ranolazine is exerted at a site that can be shared with voltage-gated Na^+ channels.

In this study, we demonstrated that in current-clamp conditions, application of ranolazine at concentration less than 3 μM produced an increase in the firing rate of APs and a concomitant conversion from an irregular to a regular discharge pattern. The present results also found that ranolazine's effect on the repetitive firing of APs tends to have biphasic concentration dependence, with low (e.g., 1 μM) concentrations producing an increase in the firing rate, while higher (10 μM) concentrations produce a reduction of AP firing. The opposite effects produced by low and high concentrations of ranolazine result from a differential sensitivity of $I_{K(IR)}$ *versus* the transient component of I_{Na} to this drug. Relatively low ($0.3-1\,\mu$M) concentrations of ranolazine were observed to reduce the amplitude of $I_{K(IR)}$. While ranolazine decreased the amplitude of $I_{K(IR)}$ with an IC_{50} value of 0.92 μM, higher concentrations of ranolazine were required to produce a depressant effect on the transient I_{Na}. Consistent with a reduction of AP firing, exposure to ranolazine at high concentrations produced a reduction in I_{Na}. These effects are not due to its action on Ca^{2+} current because $I_{Ca,L}$ remained unaltered when cells were exposed to this drug. Our results from experiments on pituitary GH_3 cells suggest that ranolazine at a lower concentration may induce prolactin secretion in vivo directly through the inhibition of $I_{K(IR)}$.

Ranolazine at a concentration less than 10 μM exerted minimal effects on $I_{Ca,L}$, $I_{K(DR)}$, $I_{K(Ca)}$, or the activity of BK_{Ca} channels. This drug exerts a relatively selective block of both $I_{K(IR)}$ and late I_{Na} in GH_3 cells. Ranolazine was also found to display a biphasic effect on the repetitive firing of APs in these cells. Depending on the concentrations tested, ranolazine produces a dual stimulatory and inhibitory effects on the firing of APs. The increase of firing frequency caused by ranolazine at low concentrations is accompanied by its inhibition of $I_{K(IR)}$, while the reduction of I_{Na} caused by ranolazine at concentrations greater than 10 μM can contribute to the decreased firing frequency. This drug may thus have clinical applications beyond its current use for chronic angina or cardiac arrhythmias. Lastly, this drug may well be useful for treatment of painful or epileptic disorders because it ability to block late I_{Na} (30, 31).

Acknowledgments

The authors would like to thank Dr. Ming-Wei Lin for technical assistance. This work was partly supported by a grant from Buddhist Dalin Tzu Chi General Hospital (DTCRD98-08), Chiayi County, Taiwan. The work in this laboratory was also supported by grants from the National Science Council (NSC-97-2320B-006-021) and the Program for Promoting Academic Excellence and Developing World Class Research Centers, Ministry of Education, Taiwan.

References

1 Nash DT, Nash SD. Ranolazine for chronic stable angina. Lancet. 2008;372:1335–1341.
2 Burashnikov A, Di Diego JM, Zygmunt AC, Belardinelli L, Antzelevitch C. Atrium-selective sodium channel block as a strategy for suppression of atrial fibrillation: differences in sodium channel inactivation between atrial and ventricles and the role of ranolazine. Circulation. 2007;116:1449–1457.
3 Fredj S, Sampson KJ, Liu H, Kass RS. Molecular basis of ranolazine block of LQT-3 mutant sodium channels: evidence for site of action. Br J Pharmacol. 2006;148:16–24.
4 Rajamani S, Shryock JC, Belardinelli L. Block of tetrodotoxin-sensitive $Na_V1.7$ and tetrodotoxin-resistant $Na_V1.8$ Na^+ channels by ranolazine. Channels (Austin). 2008;2:449–460.
5 Zaza A, Belardinelli L, Shryock JC. Pathophysiology and pharmacology of the cardiac "late sodium current". Pharmacol Ther. 2008;119:326–339.
6 Noble D. Computational models of the heart and their use in assessing the actions of drugs. J Pharmacol Sci. 2008;107:107–117.
7 Wang GK, Calderon J, Wang SY. State- and use-dependent block of muscle Nav1.4 and neuronal Nav1.7 voltage-gated Na^+ channel isoforms by ranolazine. Mol Pharmacol. 2008;73:940–948.
8 Wang YJ, Lin MW, Lin AA, Wu SN. Riluzole-induced block of voltage-gated Na^+ current and activation of BK_{Ca} channels in cultured differentiated human skeletal muscle cells. Life Sci. 2008;82:11–20.
9 Wu SN, Li HF, Chiang HT. Vinpocetine-induced stimulation of calcium-activated potassium currents in rat pituitary GH_3 cells. Biochem Pharmacol. 2001;61:877–892.
10 Bauer CK, Wulfsen I, Schäfer R, Glassmeier G, Wimmers S, Flitsch J, et al. HERG K^+ currents in human prolactin-secreting adenoma cells. Pflügers Arch. 2003;445:589–600.
11 Gullo F, Ales E, Rosati B, Lecchi M, Masi A, Guasti L, et al. ERG K^+ channel blockade enhances firing and epinephrine secretion in rat chromaffin cells: the missing link to LQT2-related sudden death? FASEB J. 2003;17:330–332.
12 Rosati B, Marchetti P, Crociani O, Lecchi M, Lupi R, Arcangeli A, et al. Glucose- and arginine-induced insulin secretion by human pancreatic β-cells: the role of HERG K^+ channels in firing and release. FASEB J. 2000;14:2601–2610.
13 Schledermann W, Wulfsen I, Schwarz JR, Bauer CK. Modulation of rat erg1, erg2, erg3 and HERG K^+ currents by thyrotropin-releasing hormone in anterior pituitary cells via the native signal cascade. J Physiol. 2001;532:143–163.
14 Wu SN, Jan CR, Li HF, Chiang HT. Characterization of inhibition by risperidone of the inwardly rectifying K^+ current in pituitary GH_3 cells. Neuropsychopharmacology. 2000;23:676–689.
15 Wu SN, Lo YK, Kuo BI, Chiang HT. Ceramide inhibits the inwardly rectifying potassium current in GH_3 lactotrophs. Endocrinology. 2001;142;4785–4794.
16 Furlan F, Taccola G, Grandolfo M, Guasti L, Arcangeli A, Nistri A, et al. ERG conductance expression modulates the excitability of ventral horn GABAergic interneurons that control rhythmic oscillations in the developing mouse spinal cord. J Neurosci. 2007;27:919–928.
17 Shepard PD, Canavier CC, Levitan ES. *Ether-a-go-go*-related gene potassium channels: what's all the buzz about? Schizophr Bull. 2007;33:1263–1269.
18 Rajamani S, Shryock JC, Belardinelli L. Rapid kinetic interaction of ranolazine with HERG K^+ current. J Cardiovasc Pharmacol. 2008;51:581–589.
19 Schram G, Zhang L, Derakhchan K, Ehrlich JR, Belardinelli L, Nattel S. Ranolazine: ion-channel blocking actions and *in vivo* electrophysiological effects. Br J Pharmacol. 2004;142:1300–1308.
20 Wang YJ, Lin MW, Lin AA, Peng H, Wu SN. Evidence for state-dependent block of DPI 201-106, a synthetic inhibitor of Na^+ channel inactivation, on delayed-rectifier K^+ current in pituitary tumor (GH_3) cells. J Physiol Pharmacol. 2008;59:409–423.
21 Allen TJ, Chapman RA. Effects of ranolazine on L-type calcium channel currents in guinea-pig single ventricular myocytes. Br J Pharmacol. 1996;118:249–254.
22 Sicouri S, Timothy KW, Zygmunt AC, Glass A, Goodrow RJ, Belardinelli L, et al. Cellular basis for the electrocardiographic and arrhythmic manifestations of Timothy syndrome: effects of ranolazine. Heart Rhythm. 2007;4:638–647.
23 Wu SN, Chiang HT, Shen AY, Lo YK. Differential effects of quercetin, a natural polyphenolic flavonoid, on L-type calcium current in pituitary tumor (GH_3) and neuronal NG108-15 cells. J Cell Physiol. 2003;195:298–308.
24 Liu YC, Wu SN. Block of *erg* current by linoleoylamide, a sleep-inducing agent, in pituitary GH_3 cells. Eur J Pharmacol. 2003;458:37–47.
25 Wu SN, Peng H, Chen BS, Wang YJ, Wu PY, Lin MW. Potent activation of large-conductance Ca^{2+}-activated K^+ channels by the diphenylurea 1-3-bis-[2-hydroxy-5-(trifluoromethyl)phenyl] urea (NS1643) in pituitary tumor (GH_3) cells. Mol Pharmacol. 2008;74:1696–1704.
26 Chandler MP, Stanley WC, Morita H, Suzuki G, Roth BA, Blackburn B, et al. Short-term treatment with ranolazine improves mechanical efficiency in dogs with chronic heart failure. Circ Res. 2002;91:278–280.
27 McCormack JG, Stanley WC, Wolff AA. Ranolazine: a novel metabolic modulator for the treatment of angina. Gen Pharmacol. 1998;30:639–645.
28 Rousseau MF, Pouleur H, Cocco G, Wolff AA. Comparative efficacy of ranolazine versus atenolol for chronic angina pectoris. Am J Cardiol. 2005;95:311–316.
29 Jerling M. Clinical pharmacokinetics of ranolazine. Clin Pharmacokinet. 2006;45:469–491.
30 Renganathan M, Dib-Hajj S, Waxman SG. $Na_V1.5$ underlies the 'third TTX-R sodium current' in rat small DRG neurons. Brain Res Mol Brain Res. 2002;106;70–82.
31 Sokolov S, Scheuer T, Catterall WA. Gating pore current in an inherited ion channelopathy. Nature. 2007;446;76–78.